Received: 26 June 2023 | Revised: 12 September 2023 | Accepted: 12 September 2023
DOI: 10.1111/gcb.16961

Global Change Biology WILEY

OPINION

Increased atmospheric CO_2 and the transit time of carbon in terrestrial ecosystems

Estefanía Muñoz[1] | **Ingrid Chanca**[1,2] | **Carlos A. Sierra**[1]

[1]Theoretical Ecosystem Ecology Group, Max Planck Institute for Biogeochemistry, Jena, Germany
[2]Laboratório de Radiocarbono, Instituto de Física, Universidade Federal Fluminense, Niterói, Brazil

Correspondence
Estefanía Muñoz, Theoretical Ecosystem Ecology Group, Max Planck Institute for Biogeochemistry, Jena, Germany.
Email: ehoyos@bgc-jena.mpg.de

Funding information
Alexander von Humboldt-Stiftung; Bundesministerium für Bildung und Forschung, Grant/Award Number: 01LK1602A; Max Planck Institute for Biogeochemistry

Abstract

The response of terrestrial ecosystems to increased atmospheric CO_2 concentrations is controversial and not yet fully understood, with previous large-scale forest manipulation experiments exhibiting contrasting responses. Although there is consensus that increased CO_2 has a relevant effect on instantaneous processes such as photosynthesis and transpiration, there are large uncertainties regarding the fate of extra assimilated carbon in ecosystems. Filling this research gap is challenging because tracing the movement of new carbon across ecosystem compartments involves the study of multiple processes occurring over a wide range of timescales, from hours to millennia. We posit that a comprehensive quantification of the effect of increased CO_2 must answer two interconnected questions: How much and for how long is newly assimilated carbon stored in ecosystems? Therefore, we propose that the transit time distribution of carbon is the key concept needed to effectively address these questions. Here, we show how the transit time distribution of carbon can be used to assess the fate of newly assimilated carbon and the timescales at which it is cycled in ecosystems. We use as an example a transit time distribution obtained from a tropical forest and show that most of the 60% of fixed carbon is respired in less than 1 year; therefore, we infer that under increased CO_2, most of the new carbon would follow a similar fate unless increased CO_2 would cause changes in the rates at which carbon is cycled and transferred among ecosystem compartments. We call for a more frequent adoption of the transit time concept in studies seeking to quantify the ecosystem response to increased CO_2.

KEYWORDS
carbon–climate feedbacks, forest ecosystems, free-air CO_2 enrichment (FACE) experiments, radiocarbon, terrestrial carbon cycle

1 | INTRODUCTION

Atmospheric CO_2 concentrations have drastically increased since the beginning of the industrial revolution, not only contributing significantly to global warming but also triggering a number of carbon–climate feedbacks that are still poorly understood (Friedlingstein et al., 2014, 2022; Schimel et al., 2015; Torn & Harte, 2006). Of particular scientific interest is the response of the terrestrial biosphere to increases in atmospheric CO_2 and temperature, and how this biospheric response would interact with the climate system. Although terrestrial vegetation draws down a large part of the CO_2 emitted by humans, it is not entirely clear what happens to this carbon fixed by the vegetation, that is where is it allocated to and for how long it remains stored in an ecosystem, and whether temperature changes may modify ecosystem metabolism and accelerate its return back to the atmosphere (Ellsworth et al., 2017; Jiang, Medlyn, et al., 2020; Klein et al., 2016; Körner et al., 2005; Norby et al., 2005; van Groenigen et al., 2014; Walker et al., 2019). There is the hypothesis that plants and forests are fertilized under increased CO_2, resulting in greater carbon assimilation through photosynthesis, which is then turned into biomass. This hypothesis is partially supported by the shape of the photosynthetic CO_2 response curve (Farquhar et al., 1980; Körner et al., 2007) that indicates a direct relationship between atmospheric CO_2 concentration and carbon assimilation, and it is also supported by experiments with CO_2 enrichment carried out at small temporal and spatial scales or in young forests (e.g. Keenan et al., 2021; Luo et al., 2003; Norby et al., 2005; Ryan, 2013). On the contrary, some studies contend that this gain in biomass does not occur at the ecosystem scale, particularly where nutrients are limited (Ellsworth et al., 2017; Fleischer et al., 2019; Fleischer & Terrer, 2022; Jiang, Caldararu, et al., 2020; Jiang, Medlyn, et al., 2020; Körner et al., 2007; Maschler et al., 2022; Xiao et al., 2022).

Free-air CO_2 enrichment (FACE) experiments have found diverse and even contradictory results. Most of the first-generation FACE experiments carried out in forest ecosystems, such as Bangor-FACE (UK), DukeFACE (USA) and AspenFACE (USA), have suggested that carbon sequestration is likely to increase as atmospheric CO_2 increases (Gustafson et al., 2020; Luo et al., 2003; Smith et al., 2013). All these forests were young and in an aggradation stage. However, FACE experiments in mature forests, such as EucFACE (Australia), BIFoR (UK) and Web-FACE (Switzerland), indicate contrasting results. In EucFACE, it was observed that aboveground productivity does not increase in response to elevated CO_2 despite a high increase in photosynthesis (Ellsworth et al., 2017), but rather that most of the extra assimilated carbon is emitted back to the atmosphere via respiratory fluxes (Jiang, Medlyn, et al., 2020). Results from Web-FACE led to similar conclusions (Körner et al., 2005), while in BIFoR, increases in belowground net primary productivity were found (Ziegler et al., 2023), suggesting a positive response to increased CO_2 in systems under the conditions of this forest, which include an adequate nutrient supply (Gardner et al., 2022).

There seems to be a consensus that increased CO_2 leads to modifications of instantaneous processes such as photosynthesis and transpiration (Fernández-Martínez et al., 2019; Huang et al., 2007; Jiang, Medlyn, et al., 2020; Paschalis et al., 2017). However, there is great uncertainty about what happens to this extra carbon once it is assimilated and converted into organic matter, that is how much is turned into long-lived biomass and how much organic carbon is quickly metabolized and respired back to the atmosphere? This uncertainty has led many scientists (e.g. De Kauwe et al., 2014; Jiang, Medlyn, et al., 2020; Körner et al., 2007) to repetitively ask the question: Where does the carbon go?

Answering this question is challenging because it implies tracing the fate of all carbon fixed during photosynthesis and following it as it moves across different types of organic compounds and vegetation tissue, tracking how it passes through food webs and other organisms and determining when it is eventually respired as part of cell metabolism from autotrophs and heterotrophs (Figure 1). All of these processes occur on a continuous range of temporal scales, from hours to days in the case of assimilation and respiration of simple photosynthates such as sugars and starch (Carbone et al., 2013; Ceballos-Núñez et al., 2018; Herrera-Ramírez et al., 2020), to centuries and millennia in the case of organic matter transfers to soil and subsequent slow decomposition (Sierra, Hoyt, et al., 2018; Trumbore, 2009; Xiao et al., 2022).

In our view, a comprehensive quantification of the effects of elevated CO_2 in ecosystems involves answering two interrelated questions: *How much* and for *how long* is carbon stored in an ecosystem?

FACE experiments are very helpful for answering both questions, but we would argue that much emphasis has been given to the question of how much extra carbon is assimilated and where it can be found at discrete measurement times. However, much less emphasis has been given to the question of how long the extra carbon remains over a continuous range of timescales.

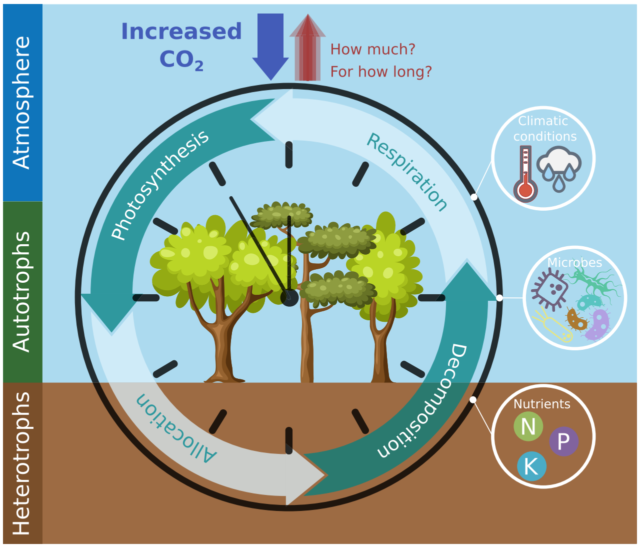

FIGURE 1 Terrestrial ecosystems remove CO_2 from the atmosphere via photosynthesis and convert it into biomass and soil organic matter. This carbon is returned to the atmosphere via decomposition and respiration, processes that depend on climatic conditions, microbial community structure and function, and nutrient availability. When ecosystems are exposed to increased CO_2, the photosynthesis rate increases, but it is not clear how much carbon remains in the system and for how long. How long carbon remains out of the atmosphere determines the consequences of increased CO_2 in ecosystems. Modified after Steiner (2008).

We claim that the transit time distribution of carbon in a terrestrial ecosystem (Bolin & Rodhe, 1973; Eriksson, 1971; Thompson & Randerson, 1999) is the key concept needed to satisfactorily address the questions of how much, where it goes and for how long the extra carbon from increased CO_2 stays in the different C pools of the ecosystem. The transit time distribution of carbon integrates the multitude of processes occurring in an ecosystem and covers a wide range of timescales (Bolin & Rodhe, 1973; Sierra, Estupinan-Suarez, et al., 2021). It is a macroscale metric that implicitly accounts for interactions resulting from the multitude of processes occurring at finer scales. For instance, it can account for the combined effect of the availability of water, energy and nutrients on carbon assimilation, allocation and respiration. As a concept, it can be incorporated into field experiments and models and could help to reconcile experiments with contrasting results.

In this manuscript, we aim to demonstrate the usefulness and robustness of the transit time concept for understanding the effects of increased CO_2 on ecosystem carbon dynamics, calling for its frequent adoption in studies that seek to quantify ecosystem response to increases in CO_2. For this purpose, we will briefly describe what transit time is and the basic equations to quantify its distribution; then, we will demonstrate through an example the usefulness of this concept, ending with the delimitation of the currently available techniques for its quantification and some final remarks.

2 | WHAT IS THE TRANSIT TIME DISTRIBUTION OF CARBON?

Transit time (τ) is a variable that characterizes the time elapsed since carbon enters the system via photosynthesis until it is released from the ecosystem through multiple processes such as autotrophic and heterotrophic respiration, leaching of dissolved organic carbon (DOC), and erosion from soils (Bolin & Rodhe, 1973; Sierra et al., 2022; Thompson & Randerson, 1999). It is equivalent to the age of the carbon in the output flux (Chanca et al., 2022), with age being defined as the time carbon is present in the ecosystem since the time of photosynthetic fixation. Because organic molecules from a cohort of carbon fixed at the same time would leave the ecosystem at different times depending on their allocation in vegetation and their fate in soils, a probability density function thus characterizes the proportions of the total amount of carbon in the output flux that passes through the ecosystem with different transit times. This distribution links three main ecosystem processes—photosynthesis, storage and respiration—because it takes into account the time at which carbon is fixed during photosynthesis, the time this carbon remains stored and when it is lost from the system. Therefore, this concept is an excellent tool for diagnosing ecosystem dynamics and their processes at the ecosystem level (Sierra, Crow, et al., 2021).

The transit time distribution of carbon is a continuous function that can be computed from any ecosystem model. It can be obtained from impulse response functions (Joos et al., 2013; Meyer et al., 1999; Thompson & Randerson, 1999), or from the analytical structure of a C cycle model expressed as a compartmental dynamical system (Metzler et al., 2018; Metzler & Sierra, 2018). In compartmental form, the carbon cycle of an ecosystem can be generalized by the nonlinear nonautonomous equation (Luo et al., 2022; Sierra, Ceballos-Núñez, et al., 2018):

$$\frac{dx}{dt} = \dot{\boldsymbol{x}}(t) = \boldsymbol{u}(\boldsymbol{x}(t), t) + \mathbf{B}(\boldsymbol{x}(t), t) \cdot \boldsymbol{x}(t), \tag{1}$$

where $\boldsymbol{x}$ is a vector expressing the content of carbon in n number of ecosystem compartments. The vector $\boldsymbol{u}$ represents the external carbon inputs to the ecosystem from the atmosphere and the matrix $\mathbf{B}$ represents the rates of carbon cycling and transfers within the ecosystem. Both $\boldsymbol{u}$ and $\mathbf{B}$ can depend on the compartment's contents $\boldsymbol{x}(t)$ and change over time t. For the most common representation of carbon dynamics in ecosystems and land surface models, that is the linear autonomous (Lu et al., 2018; Metzler & Sierra, 2018; Sierra, Estupinan-Suarez, et al., 2021), Equation (1) reduces to the compartmental system $\dot{\boldsymbol{x}}(t) = \boldsymbol{u} + \mathbf{B}\boldsymbol{x}(t)$, and the transit time distribution in equilibrium has the solution:

$$f(\tau) = -\mathbf{1}^{\mathsf{T}}\ \mathbf{B}\ e^{\tau \mathbf{B}}\ \frac{\boldsymbol{u}}{\| \boldsymbol{u} \|}, \tag{2}$$

where the symbol $\| \cdot \|$ represents the sum of all elements inside the vector $\boldsymbol{u}$, and $_{\mathsf{T}}$ represents the transpose of the vector containing ones. The mean or expected value of the transit time is:

$$\mathbb{E}(\tau) = -\mathbf{1}^{\mathsf{T}}\mathbf{B}^{-1}\frac{\mathbf{u}}{\| \mathbf{u} \|}. \tag{3}$$

The mathematical expressions of the steady state of the linear autonomous case are detailed in Appendix A, and the procedure for applying the transit time concept to any combination of t-dependence and x-dependence conditions, provided the carbon cycle is represented as a compartmental system, is described in Metzler et al. (2018).

The transit time distribution of carbon in an ecosystem at equilibrium (Equation 2) expresses the proportion of carbon in the output flux with transit time τ. Because the matrix $\mathbf{B}$ encodes all the information regarding how fast carbon is processed and transferred among the different compartments, $f(\tau)$ captures all the different paths that a particle of carbon could take to travel through an ecosystem and how much time it would spend stored. Extra new carbon entering an ecosystem as a result of increased CO_2 would also have a path across ecosystem compartments until it is lost. The transit time of this carbon would then indicate the proportion of new extra carbon that would remain stored in biomass and other ecosystem compartments at decadal or longer timescales, as well as the proportions of new carbon that would be assimilated quickly and respired back to the atmosphere at daily or intra-annual timescales. In the next section, we will use a transit time distribution of carbon obtained from a tropical forest to evaluate the range of timescales at which carbon is lost from this ecosystem.

3 | THE TRANSIT TIME DISTRIBUTION OF CARBON AND THE FATE OF CARBON UNDER INCREASED CO_2

To illustrate the potential of the transit time approach to quantify the effects of increased CO_2 on ecosystem carbon dynamics at different timescales, we use as a theoretical example the ecosystem model obtained for the tropical forests of the Porce region in Colombia, developed by Sierra, Estupinan-Suarez, et al. (2021) using a large data set of observations of carbon stocks. This is a tropical old-growth forest, so the representation of its carbon dynamics by a linear autonomous compartmental system with a solution given by Equation (2) is quite realistic. The model has seven pools: foliage, wood, fine roots, coarse roots, fine litter, coarse woody debris and soil carbon up to 30 cm depth. Gross primary productivity is approximately $23.98 \pm 2.36\,\mathrm{MgC\,ha^{-1}\,year^{-1}}$, and the values of cycling rates (matrix **B**) are those shown in table 2 in Sierra, Estupinan-Suarez, et al. (2021). The code is available in the Zenodo repository (Muñoz et al., 2023).

The probability density distribution (pdf) of the ecosystem transit time (black curve in Figure 2a) has a median ($\tilde{\tau}$) of 0.5 years, indicating that most of the metabolic processes responsible for maintaining organic tissue operate at short timescales, with 50% of the carbon being lost in half a year after fixation. Figure 2a also shows that the transit time pdf of each ecosystem pool has different shapes, contributing to different proportions of the overall distribution. The distribution of the soil carbon pool has a long tail, implying that a very small proportion of carbon in soil may remain for hundreds of years. This contrasts with carbon in foliage, which returns back to the atmosphere very rapidly, in timescales from days to months. The transit time distribution shows that 50% of the carbon from the foliage is lost in 0.2 years, while in the soil, half of the stored carbon returns in 41.1 years. However, most of the carbon in the ecosystem is lost through fast pools, such as foliage and fine litter, making its $\tilde{\tau}$ more similar to those of these pools than to slow pools, such as soil carbon and coarse roots.

Figure 2b represents the probability that the carbon that entered the ecosystem at time t_0 (fixation time) will be released after a time greater than or equal to T has elapsed; in other words, the probability that the carbon has not yet been respired at time T. These bars correspond to the integral under the curves representing each pool shown in Figure 2a at the discrete times corresponding to 1, 5, 20, 50 and 100 years, and suggest that at each T, the probability that carbon from each pool remains still in the system is very different, contributing diversely to the carbon dynamics of the entire ecosystem. As expected from Figure 2a, at short timescales (1 year), most of the carbon from foliage has already been respired, and only ≈5.1% will be released later, rendering its contribution insignificant. Something similar occurs with the carbon in the fine litter, which is mostly respired before 1 year (≈73.6%). At longer timescales, the probability decreases significantly, with almost all carbon being respired 100 years after fixation, except for ≈14.5% from the soil, ≈10.8% from the coarse roots and ≈6.7% from fine roots. Furthermore, Figure 2b shows how the dynamics of the entire ecosystem are driven by what happens in each pool differently over time, with the probability of carbon being already respired at 1 year of ≈67.2% and after 100 years of ≈2.2%.

Figure 2 demonstrates how the transit time concept is able to provide information about how carbon fixed during photosynthesis returns to the atmosphere over a wide range of temporal scales, capturing the fast dynamics of respiratory processes and the slow dynamics of carbon transfers among pools and carbon stabilization in soils (Ceballos-Núñez et al., 2018; Herrera-Ramírez et al., 2020; Sierra, Estupinan-Suarez, et al., 2021). Intuitively, the transit time distribution of carbon for this tropical forest suggests that new extra carbon from increased CO_2 would also be lost very quickly

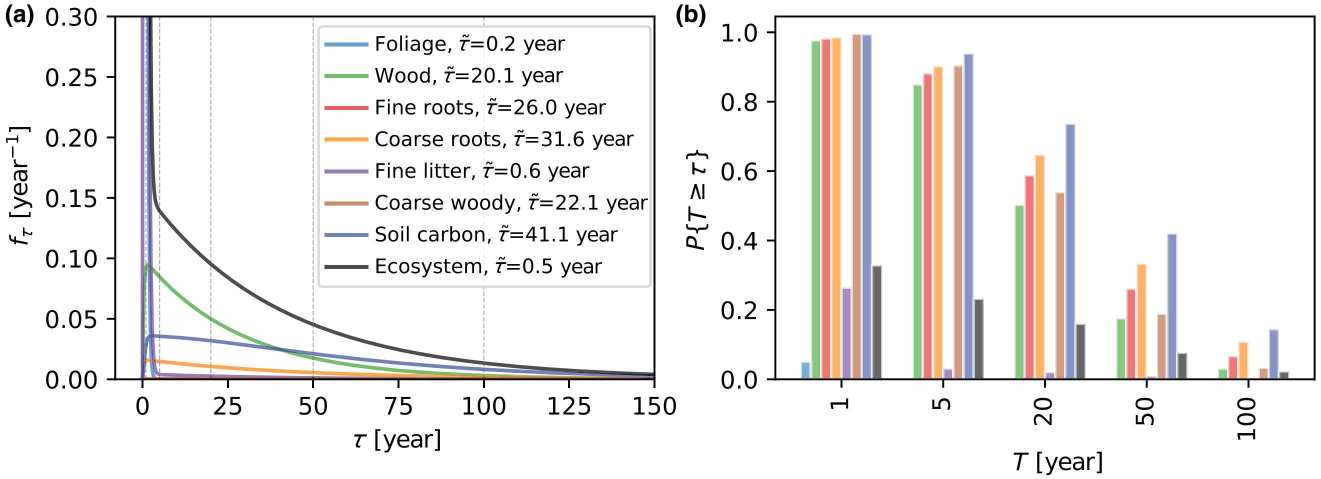

FIGURE 2 Transit time density distributions of the ecosystem and each pool (a), and the probability that carbon that entered the ecosystem at t_0 has not been yet respired at times T (b). The dotted grey vertical lines in (a) represent the discrete times at which it is integrated in (b). The colours in both panels indicate the different pools, as described in the legend of (a). Note that the density curve of the coarse woody pool in (a) is difficult to see because it is so close to zero.

after fixation, and only very small proportions would be stored and detectable at longer timescales.

Imitating a CO_2 fertilization experiment that increases photosynthesis rates, as found by different authors (e.g. Fernández-Martínez et al., 2019; Keenan et al., 2021), we multiply the vector $\boldsymbol{u}$ by a factor γ ($\gamma=1$, 2 and 3), increasing carbon inputs by 200% and 300%. These γ values were chosen to illustrate what happens to carbon dynamics for very high increases in carbon inputs such as those evaluated in fertilization experiments. The resulting transit time mass distributions and transit time pdfs are shown in Figure 3a,b and indicate that, as in Figure 2a, most carbon is rapidly lost within the first few years after photosynthetic fixation, even with very high carbon inputs. Increasing carbon inputs, steady-state carbon stock increases by the same proportion $\left(-\mathbf{B}^{-1}(\gamma\mathbf{u}) = \gamma\left(-\mathbf{B}^{-1}\mathbf{u}\right)\right)$; however, so does respired carbon (Figure 3a). In other words, the behaviour of one unit of assimilated carbon is the same independent of how much photosynthesis increases by the proportion γ (Figure 3b), so this unit of carbon stays in the ecosystem for the same amount of time regardless of how much carbon entered in the first place. This can be confirmed mathematically by the mean transit time expression in Equation (4) (Sierra, Crow, et al., 2021), where γ cancels out from the expression in Equation (3).

$$\mathbb{E}(\tau) = -\mathbf{1}^{\mathsf{T}}\mathbf{B}^{-1}\frac{\gamma\mathbf{u}}{\|\gamma\mathbf{u}\|}. \tag{4}$$

This leads us to ask: What is necessary for the probability density function of transit time distribution to change, causing the ecosystem to retain extra carbon for longer? The other component of the carbon balance (Equation 1) that can be modified besides the inputs is the one associated with matrix $\mathbf{B}$, which contains the cycling and transfer rates within the ecosystem and between the ecosystem and the atmosphere. Rates of ecosystem carbon cycling usually change due to environmental factors such as nitrogen or phosphorus availability, temperature or water availability, among others (Hutchinson et al., 2007; Schimel et al., 2015; Zaehle et al., 2014). To test the effect of modifications on these rates, we multiply matrix $\mathbf{B}$ by ξ ($\xi=0.5$, 1.0, 1.5) for the case where CO_2 fertilization has increased carbon inputs by 200% ($\gamma=2$). When $\xi<1$ ($\xi>1$), the distribution tails (Figure 3c,d) become heavier (lighter); therefore, carbon stays longer (shorter) in the ecosystem. More importantly, variations of ξ in $\mathbf{B}$ not only proportionally change carbon storage $\left(-(\xi\mathbf{B})^{-1}\mathbf{u} = \frac{1}{\xi}\left(-\mathbf{B}^{-1}\mathbf{u}\right)\right)$, but also transit times, changing the mean of τ according to Equation (5), and, consequently, the behaviour of one unit of assimilated carbon (Figure 3d).

$$\frac{\mathbb{E}(\tau)}{\xi} = -\mathbf{1}^{\mathsf{T}}(\xi\mathbf{B})^{-1}\frac{\mathbf{u}}{\|\mathbf{u}\|}. \tag{5}$$

These results suggest that it is not the increase in carbon assimilation induced by increases in CO_2 by itself that would change the dynamics of the time carbon spends in ecosystems, but rather potential associated changes in the fate of the assimilated carbon and the rates at which it is processed inside ecosystem compartments. Such ecosystem changes may include changes in the chemistry of organic matter and the rates at which it is decomposed from soils, changes in C allocation patterns in plants, for example more C allocated to roots than foliage; or changes in plant and microbial communities that would process carbon at different rates. In combination, these ecosystem changes may generate changes in carbon storage and respiration that would affect the time carbon spends in each pool ($\tilde{\tau}$ induced by changes in ξ). Although

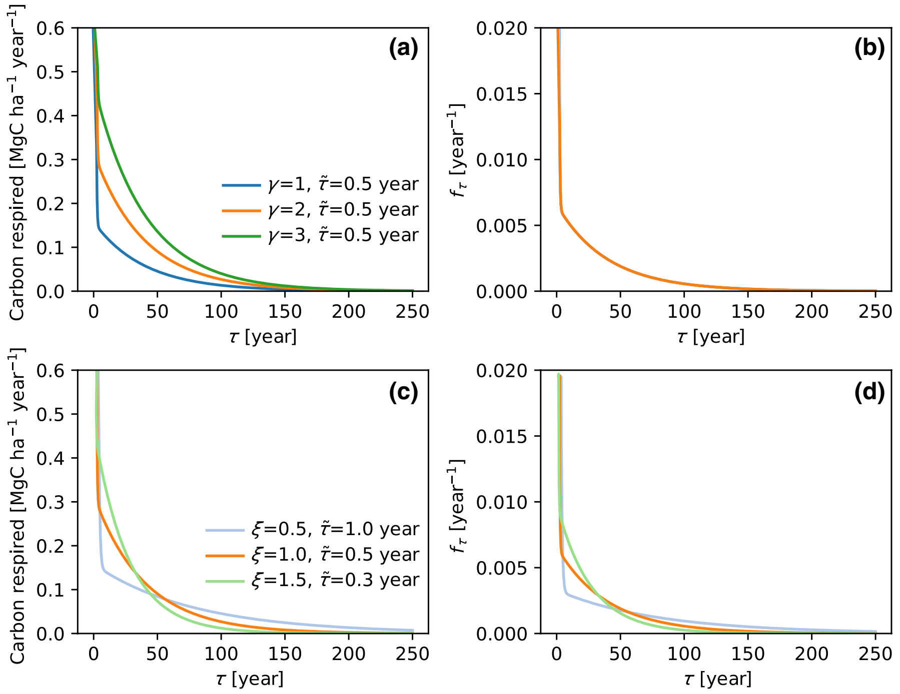

FIGURE 3 Transit time mass distribution (left panel (a,c)) and probability density distributions (right panel (b,d)) when modifying the carbon inputs ($\boldsymbol{u}$) by γ (upper panel (a,b)) and matrix $\mathbf{B}$ by ξ (for $\gamma=2$) (bottom panel (c,d)). The colours represent the values of γ and ξ, and $\tilde{\tau}$ is the median of the transit time.

these results are valid for systems in equilibrium, they give insights into what could occur in systems out of equilibrium (Sierra, Crow, et al., 2021).

Figure 3 demonstrates how the transit time approach helps to infer the response of ecosystem carbon dynamics to rises in CO_2 concentrations over a wide range of conditions and timescales, as well as the effects of other ecosystem processes that modify the rates of carbon cycling and the time carbon stays in ecosystem pools (e.g. water, temperature and nutrients), which are encoded in matrix **B**.

4 | HOW CAN THE CARBON TRANSIT TIME APPROACH BE IMPLEMENTED?

In this section, we briefly describe currently available techniques for obtaining the carbon transit time of an ecosystem. These techniques can be divided into modelling, induced tracers and natural tracers, defining as tracers any substance that allows us to follow and infer carbon dynamics within an ecosystem, analogous to the definition in hydrology (Benettin et al., 2022). Although these techniques can be used independently, they complement each other.

4.1 | Modelling

In general, carbon cycle models are based on mass balance equations expressed as ordinary differential equations (e.g. Equation 1) from which transit time distributions can be obtained.

Thompson and Randerson (1999) and Manzoni et al. (2009) used the impulse response function approach to calculate the transit time distribution for linear and autonomous models with multiple pools. Thompson and Randerson (1999) computed the pdfs numerically by long-term simulations while Manzoni et al. (2009) used the Laplace transform to explicitly obtain the system response function of models with simple structures. The derivation of the Laplace transform for more complex models is not always possible with the full set of equations of large models.

Other authors (e.g. Metzler et al., 2018; Metzler & Sierra, 2018; Rasmussen et al., 2016) have made use of compartmental models (Sierra, Ceballos-Núñez, et al., 2018) to describe the temporal dynamics of carbon travelling through the ecosystem compartments. Rasmussen et al. (2016) developed efficient computational equations for linear and nonautonomous compartmental systems that describe the temporal evolution of the mean transit time; however, they do not allow the calculation of the complete distribution. Metzler and Sierra (2018) proposed explicit formulas for transit time distributions of autonomous and non-linear steady-state systems expressed as continuous-time Markov chains. Most previous approaches had been concerned with time-independent equilibrium models, but a new set of techniques for dealing with time-dependent systems has recently been introduced (Chappelle et al., 2023; Metzler et al., 2018; Rasmussen et al., 2016).

Additionally, developments in disciplines such as hydrology have reached meaningful advancements for obtaining equations for complex hydrological systems out of equilibrium (e.g. Benettin et al., 2022; Botter et al., 2011; Calabrese & Porporato, 2015; Kirchner, 2019) that may be useful for deriving algorithms to model non-linear and nonautonomous dynamics in the C cycle. This discipline has the advantage of a well-developed approach to tracing isotopes to infer water age, as well as a large number of isotope records. However, hydrological models have mainly focussed on a single compartment (watershed water storage) with two or three output fluxes (evaporation, transpiration and flow out of a catchment).

4.2 | Induced tracers

Isotopic labelling techniques have been applied successfully in plant ecology and soil science over the previous decades, mostly to understand rates of C transfer among plant or soil compartments, cycling rates of individual compartments or the identification of distinct timescales of C cycling associated with plant or soil metabolism (Epron et al., 2012). Due to logistical constraints, pulse labelling experiments have been conducted predominantly with small (potted) plants, tree organs such as branches or incubated soil samples under laboratory conditions. Nevertheless, there are already a few studies with pulse labelling of entire ecosystems such as grasslands (Riederer et al., 2015) or entire forest ecosystems under controlled environments such as those in Biosphere 2 (Werner et al., 2021).

Pulse response experiments at the ecosystem scale, monitoring the trajectory of the label in the total respiration flux, offer the best opportunity to obtain empirically a transit time distribution. In old-growth ecosystems where photosynthetic C inputs are nearly balanced with respiration outputs, the temporal dynamics of a tracer follow linear dynamics even when there are non-linear interactions among ecosystem components (Anderson, 2013; Metzler & Sierra, 2018). For these systems, the temporal dynamics of the tracer in the output flux provides an approximation to the transit time distribution function of Equation (2). Furthermore, if the release of the tracer from individual compartments such as foliage, stems or soil carbon is monitored over time, the resulting curves should be equivalent to the components of the transit time distribution presented in Figure 2a.

Curves describing the dynamics of a pulse label in ecosystem respiration offer the best opportunity to infer the fate of increased CO_2 in ecosystems. They provide information on how long new carbon stays in an ecosystem and what proportions of C will be stored for longer timescales and respired years or decades later. Available information from pulse labelling experiments consistently shows a maximum peak of the tracer in respiration a few days after injection (Epron et al., 2012; Werner et al., 2021), suggesting that most carbon entering ecosystems is respired quickly after assimilation. The tail of the pulse response curve provides information on the proportion of assimilated carbon that remains stored in the ecosystem for long timescales, and, in general, the available data show that only very small proportions of the label can be detected weeks or months later (Werner et al., 2021).

4.3 | Natural tracer

Radiocarbon (^{14}C) is a natural radioactive isotope of carbon. Alongside its cosmogenic natural production, a large amount of ^{14}C was produced in the atmosphere during the 1950s and early 1960s as a by-product of thermonuclear weapons tests (bomb effect). This excess ^{14}C led to a disequilibrium between $^{14}C/C$ ratio in the atmosphere, biosphere and surface ocean (Levin et al., 2022), which has been used to trace the dynamics of C cycling in terrestrial pools as well as in oceans (Beaupré & Druffel, 2009; Shi et al., 2020). Additionally, ^{14}C measurements in forest CO_2 have been used to estimate the mean age of ecosystem respiration (Phillips et al., 2015).

Natural tracers such as radiocarbon have the advantage of continuously introducing a signature that can be tracked independently of when a field experiment or data collection may start. Since the $^{14}C/^{12}C$ ratio—in $\Delta^{14}C$ notation (Stuiver & Polach, 1977)—is corrected for mass-dependent fractionation, $\Delta^{14}C$ informs about the time that carbon of certain signature in the atmosphere takes to appear in ecosystem output fluxes such as respiration or DOC leachate. The incorporation of ^{14}C by ecosystem compartments follows the same dynamics as C incorporation in individual compartments, with fast cycling compartments such as foliage exchanging ^{14}C very quickly with the atmosphere, and slow cycling compartments accumulating a wide range of $\Delta^{14}C$ values (Chanca et al., 2022). Long-lived compartments such as mineral associated soil C may also include the radiocarbon signature of ^{14}C-depleted carbon due to radioactive decay. In this sense, the radiocarbon signature of the output fluxes would contain a broad mix of $\Delta^{14}C$ that can also be characterized by a probability density function (Chanca et al., 2022).

FACE experiments often create a unique opportunity to use the injected CO_2 in treatment plots to trace the dynamics of carbon isotopes (Hopkins et al., 2012; Leavitt et al., 1994, 1995). The CO_2 from tanks routinely used to enhance the atmospheric CO_2 concentrations in FACE experiments can induce a contribution of ^{14}C-free masses to treatment plots, which can be used to derive the transit time distributions if the isotopic concentrations are continuously measured in output fluxes.

As mentioned above, the three methods described in this section are complementary. Tracers, both natural and induced, provide independent measurement-based information that permits the identification of the model structure and its parameterization (Epron et al., 2012). Furthermore, tracers would confirm model predictions of transit time distributions (Shi et al., 2020; Sierra, Crow, et al., 2021) and would be useful in model calibration when its parameterization was performed using ecosystem biomass stocks.

Radiocarbon measurements can be taken from the different pools in the ecosystem, as well as from the air respired throughout the ecosystem, making it possible to compare the radiocarbon signature in the pools and their outfluxes, obtaining insights into the number and size of pools and the interconnections among them that better represent ecosystem dynamics (Shi et al., 2020; Sierra et al., 2017; Wang et al., 2019), thus reducing uncertainties in model predictions.

Furthermore, FACE experiments usually add CO_2 with a specific isotopic signature, essentially making them isotopic labelling experiments. As in most cases, the added CO_2 is of fossil–fuel origin, devoted to radiocarbon and with a specific signature of ^{13}C, data from the FACE experiments can also be analysed as a tracer experiment and, together with a model tracing the isotope, transit time distributions can be obtained.

5 | CONCLUDING REMARKS AND IMPLICATIONS

The transit time distribution of carbon provides key information to understand the effects of increased CO_2 in terrestrial ecosystems (Figure 4a). It captures information about the fate of newly assimilated carbon, allowing us to trace how much and for how long new carbon is stored in an ecosystem over a wide range of timescales. We believe this concept is essential to infer the consequences of human-induced increases in atmospheric CO_2 concentrations on the carbon balance of the terrestrial biosphere (Figure 4b). Because the distribution integrates multiple ecosystem processes, it permits the study of future scenarios of fossil fuel emissions that lead to different trajectories of CO_2 concentrations, and potential interactions with other factors such as nutrient and water availability that may modify internal ecosystem process rates (as represented in matrix **B**).

Previous estimates of transit time distributions of carbon in terrestrial ecosystems using models or isotopic tracers (Sierra, Estupinan-Suarez, et al., 2021; Thompson & Randerson, 1999; Werner et al., 2021) suggest that this distribution is a mix of exponential distributions and that, in mature forests, most carbon fixed by photosynthesis at any given time is lost quickly and does not remain stored for long timescales. Therefore, one would conclude from these previous studies that under increased CO_2 most of the extra carbon will be respired and returned to the atmosphere at short timescales (<1 year), and the remaining C that could stay stored in long-term C pools may be difficult to detect, particularly in FACE experiments lasting a few years. This is a potential explanation for results from previous experiments such as those of Ellsworth et al. (2017) and Jiang, Medlyn, et al. (2020) where most of the extra carbon was lost in increased ecosystem respiration. However, if increased CO_2 leads to increased biomass and carbon accumulation, then important changes in transfer and cycling rates of carbon among ecosystem compartments (as encoded in matrix **B**) must be responsible for differences in ecosystem carbon balances concerning non-CO_2-fertilized sites. In either case, the transit time distribution provides the key information for inferring the potential impacts of increased CO_2 in ecosystems. The forthcoming AmazonFACE project in a mature tropical forest located in Brazil has among its objectives to know the duration of CO_2 fertilization effect (Moutinho, 2022), providing

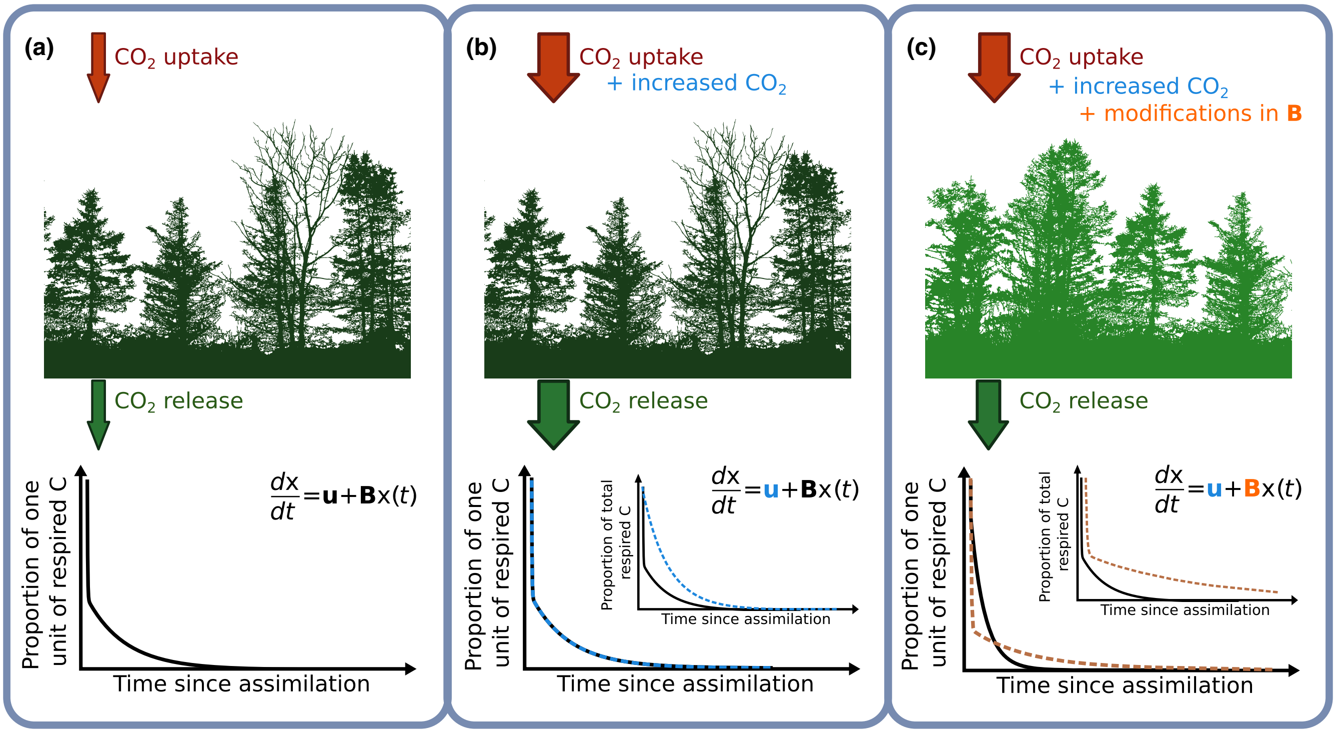

FIGURE 4 Conceptual shapes of the transit time distributions in response to increased CO$_2$ and potential modifications of other ecosystem processes. (a) Transit time distribution for an ecosystem at equilibrium. (b) Transit time distribution under increased CO$_2$ (blue dashed line) for the total amount of respired C (inset) and for one unit of respired C. Notice that both curves with and without increased CO$_2$ overlap. (c) Transit time distribution when assuming that increased CO$_2$ modifies ecosystem cycling and transfer rates, in which case new extra carbon may stay longer in an ecosystem.

a perfect opportunity to implement this concept and compare the results with those obtained in the Colombian tropical forest used in this paper to illustrate the transit time approach.

AUTHOR CONTRIBUTIONS

Estefanía Muñoz: Conceptualization; formal analysis; funding acquisition; methodology; writing – original draft; writing – review and editing. **Ingrid Chanca:** Conceptualization; methodology; writing – original draft; writing – review and editing. **Carlos A. Sierra:** Conceptualization; methodology; writing – original draft; project administration; supervision; writing – review and editing.

ACKNOWLEDGEMENTS

Funding was provided by the Alexander von Humboldt Foundation and the Max Planck Institute for Biogeochemistry. Open Access funding enabled and organized by Projekt DEAL.

CONFLICT OF INTEREST STATEMENT

The authors declare that they have no conflicts of interest.

DATA AVAILABILITY STATEMENT

The data and code supporting the example in Section 3 are publicly available in Zenodo at https://zenodo.org/record/8344936, reference number 8344936.

ORCID

Estefanía Muñoz https://orcid.org/0000-0002-5089-3316
Ingrid Chanca https://orcid.org/0000-0003-0933-5838
Carlos A. Sierra https://orcid.org/0000-0003-0009-4169

REFERENCES

Anderson, D. H. (2013). *Compartmental modeling and tracer kinetics* (Vol. 50). Springer Science & Business Media.

Beaupré, S. R., & Druffel, E. R. (2009). Constraining the propagation of bomb-radiocarbon through the dissolved organic carbon (DOC) pool in the northeast pacific ocean. *Deep Sea Research Part I: Oceanographic Research Papers*, *56*, 1717–1726. https://doi.org/10.1016/j.dsr.2009.05.008

Benettin, P., Rodriguez, N. B., Sprenger, M., Kim, M., Klaus, J., Harman, C. J., van der Velde, Y., Hrachowitz, M., Botter, G., McGuire, K. J., Kirchner, J. W., Rinaldo, A., & McDonnell, J. J. (2022). Transit time estimation in catchments: Recent developments and future directions. *Water Resources Research*, *58*, 1–36. https://doi.org/10.1029/2022WR033096

Bolin, B., & Rodhe, H. (1973). A note on the concepts of age distribution and transit time in natural reservoirs. *Tellus*, *25*, 58–62. https://doi.org/10.3402/tellusa.v25i1.9644

Botter, G., Bertuzzo, E., & Rinaldo, A. (2011). Catchment residence and travel time distributions: The master equation. *Geophysical Research Letters*, *38*, 1–6. https://doi.org/10.1029/2011GL047666

Calabrese, S., & Porporato, A. (2015). Linking age, survival, and transit time distributions. *Water Resources Research*, *51*, 8316–8330. https://doi.org/10.1002/2015WR017785

Carbone, M. S., Czimczik, C. I., Keenan, T. F., Murakami, P. F., Pederson, N., Schaberg, P. G., Xu, X., & Richardson, A. D. (2013). Age, allocation and availability of nonstructural carbon in mature red maple trees. *New Phytologist*, *200*, 1145–1155. https://doi.org/10.1111/nph.12448

Ceballos-Núñez, V., Richardson, A. D., & Sierra, C. A. (2018). Ages and transit times as important diagnostics of model performance for predicting carbon dynamics in terrestrial vegetation models. *Biogeosciences*, *15*, 1607–1625. https://doi.org/10.5194/bg-15-1607-2018

Chanca, I., Trumbore, S., Macario, K., & Sierra, C. A. (2022). Probability distributions of radiocarbon in open linear compartmental systems at steady-state. *Journal of Geophysical Research: Biogeosciences*, *127*, e2021JG006673. https://doi.org/10.1029/2021jg006673

Chappelle, G., Hastings, A., & Rasmussen, M. (2023). Pool dynamics of time-dependent compartmental systems with application to the terrestrial carbon cycle. *Journal of the Royal Society Interface*, *20*, 20220843. https://doi.org/10.1098/rsif.2022.0843

De Kauwe, M. G., Medlyn, B. E., Zaehle, S., Walker, A. P., Dietze, M. C., Wang, Y. P., Luo, Y., Jain, A. K., El-Masri, B., Hickler, T., Wårlind, D., Weng, E., Parton, W. J., Thornton, P. E., Wang, S., Prentice, I. C., Asao, S., Smith, B., Mccarthy, H. R., … Norby, R. J. (2014). Where does the carbon go? A model-data intercomparison of vegetation carbon allocation and turnover processes at two temperate forest free-air CO$_2$ enrichment sites. *New Phytologist*, *203*, 883–899. https://doi.org/10.1111/nph.12847

Ellsworth, D. S., Anderson, I. C., Crous, K. Y., Cooke, J., Drake, J. E., Gherlenda, A. N., Gimeno, T. E., Macdonald, C. A., Medlyn, B. E., Powell, J. R., Tjoelker, M. G., & Reich, P. B. (2017). Elevated CO$_2$ does not increase eucalypt forest productivity on a low-phosphorus soil. *Nature Climate Change*, *7*, 279–282. https://doi.org/10.1038/nclimate3235

Epron, D., Bahn, M., Derrien, D., Lattanzi, F. A., Pumpanen, J., Gessler, A., Högberg, P., Maillard, P., Dannoura, M., Gérant, D., & Buchmann, N. (2012). Pulse-labelling trees to study carbon allocation dynamics: A review of methods, current knowledge and future prospects. *Tree Physiology*, *32*, 776–798. https://doi.org/10.1093/treephys/tps057

Eriksson, E. (1971). Compartment models and reservoir theory. *Annual Review of Ecology and Systematics*, *2*, 67–84.

Farquhar, G. D., von Caemmerer, S., & Berry, J. A. (1980). A biochemical model of photosynthetic CO$_2$ assimilation in leaves of C3 species. *Planta*, *149*, 78–90. https://doi.org/10.1007/BF00386231

Fernández-Martínez, M., Sardans, J., Chevallier, F., Ciais, P., Obersteiner, M., Vicca, S., Canadell, J. G., Bastos, A., Friedlingstein, P., Sitch, S., Piao, S. L., Janssens, I. A., & Peñuelas, J. (2019). Global trends in carbon sinks and their relationships with CO$_2$ and temperature. *Nature Climate Change*, *9*, 73–79. https://doi.org/10.1038/s41558-018-0367-7

Fleischer, K., Rammig, A., De Kauwe, M. G., Walker, A. P., Domingues, T. F., Fuchslueger, L., Garcia, S., Goll, D. S., Grandis, A., Jiang, M., Haverd, V., Hofhansl, F., Holm, J. A., Kruijt, B., Leung, F., Medlyn, B. E., Mercado, L. M., Norby, R. J., Pak, B., … Lapola, D. M. (2019). Amazon forest response to CO$_2$ fertilization dependent on plant phosphorus acquisition. *Nature Geoscience*, *12*, 736–741. https://doi.org/10.1038/s41561-019-0404-9

Fleischer, K., & Terrer, C. (2022). Estimates of soil nutrient limitation on the CO$_2$ fertilization effect for tropical vegetation. *Global Change Biology*, *28*, 6366–6369. https://doi.org/10.1111/gcb.16377

Friedlingstein, P., Jones, M. W., O'Sullivan, M., Andrew, R. M., Bakker, D. C. E., Hauck, J., Le Quéré, C., Peters, G. P., Peters, W., Pongratz, J., Sitch, S., Canadell, J. G., Ciais, P., Jackson, R. B., Alin, S. R., Anthoni, P., Bates, N. R., Becker, M., Bellouin, N., … Zeng, J. (2022). Global carbon budget 2021. *Earth System Science Data*, *14*, 1917–2005. https://doi.org/10.5194/essd-14-1917-2022

Friedlingstein, P., Meinshausen, M., Arora, V. K., Jones, C. D., Anav, A., Liddicoat, S. K., & Knutti, R. (2014). Uncertainties in CMIP5 climate projections due to carbon cycle feedbacks. *Journal of Climate*, *27*, 511–526. https://doi.org/10.1175/JCLI-D-12-00579.1

Gardner, A., Ellsworth, D. S., Crous, K. Y., Pritchard, J., & Mackenzie, A. R. (2022). Is photosynthetic enhancement sustained through three years of elevated CO$_2$ exposure in 175-year-old *Quercus robur*? *Tree Physiology*, *42*, 130–144. https://doi.org/10.1093/treephys/tpab090

Gustafson, E. J., Miranda, B. R., & Sturtevant, B. R. (2020). How do forest landscapes respond to elevated CO$_2$ and ozone? Scaling Aspen-FACE plot-scale experimental results. *Ecosphere*, *11*, 3162. https://doi.org/10.1002/ecs2.3162

Herrera-Ramírez, D., Muhr, J., Hartmann, H., Römermann, C., Trumbore, S., & Sierra, C. A. (2020). Probability distributions of nonstructural carbon ages and transit times provide insights into carbon allocation dynamics of mature trees. *New Phytologist*, *226*, 1299–1311. https://doi.org/10.1111/nph.16461

Hopkins, F. M., Torn, M. S., & Trumbore, S. E. (2012). Warming accelerates decomposition of decades-old carbon in forest soils. *Proceedings of the National Academy of Sciences of the United States of America*, *109*, E1753–E1761. https://doi.org/10.1073/pnas.1120603109

Huang, J. G., Bergeron, Y., Denneler, B., Berninger, F., & Tardif, J. (2007). Response of forest trees to increased atmospheric CO$_2$. *Critical Reviews in Plant Sciences*, *26*, 265–283. https://doi.org/10.1080/07352680701626978

Hutchinson, J. J., Campbell, C. A., & Desjardins, R. L. (2007). Some perspectives on carbon sequestration in agriculture. *Agricultural and Forest Meteorology*, *142*, 288–302. https://doi.org/10.1016/j.agrformet.2006.03.030

Jiang, M., Caldararu, S., Zhang, H., Fleischer, K., Crous, K. Y., Yang, J., De Kauwe, M. G., Ellsworth, D. S., Reich, P. B., Tissue, D. T., Zaehle, S., & Medlyn, B. E. (2020). Low phosphorus supply constrains plant responses to elevated CO$_2$: A meta-analysis. *Global Change Biology*, *26*, 5856–5873. https://doi.org/10.1111/gcb.15277

Jiang, M., Medlyn, B. E., Drake, J. E., Duursma, R. A., Anderson, I. C., Barton, C. V., Boer, M. M., Carrillo, Y., Castañeda-Gómez, L., Collins, L., Crous, K. Y., De Kauwe, M. G., dos Santos, B. M., Emmerson, K. M., Facey, S. L., Gherlenda, A. N., Gimeno, T. E., Hasegawa, S., Johnson, S. N., … Ellsworth, D. S. (2020). The fate of carbon in a mature forest under carbon dioxide enrichment. *Nature*, *580*, 227–231. https://doi.org/10.1038/s41586-020-2128-9

Joos, F., Roth, R., Fuglestvedt, J. S., Peters, G. P., Enting, I. G., von Bloh, W., Brovkin, V., Burke, E. J., Eby, M., Edwards, N. R., Friedrich, T., Frölicher, T. L., Halloran, P. R., Holden, P. B., Jones, C., Kleinen, T., Mackenzie, F. T., Matsumoto, K., Meinshausen, M., … Weaver, A. J. (2013). Carbon dioxide and climate impulse response functions for the computation of greenhouse gas metrics: A multi-model analysis. *Atmospheric Chemistry and Physics*, *13*, 2793–2825. https://doi.org/10.5194/acp-13-2793-2013

Keenan, T. F., Luo, X., De Kauwe, M. G., Medlyn, B. E., Prentice, I. C., Stocker, B. D., Smith, N. G., Terrer, C., Wang, H., Zhang, Y., & Zhou, S. (2021). A constraint on historic growth in global photosynthesis due to increasing CO$_2$. *Nature*, *600*, 253–258. https://doi.org/10.1038/s41586-021-04096-9

Kirchner, J. W. (2019). Quantifying new water fractions and transit time distributions using ensemble hydrograph separation: Theory and benchmark tests. *Hydrology and Earth System Sciences*, *23*, 303–349. https://doi.org/10.5194/hess-23-303-2019

Klein, T., Bader, M. K., Leuzinger, S., Mildner, M., Schleppi, P., Siegwolf, R. T., & Körner, C. (2016). Growth and carbon relations of mature *Picea abies* trees under 5 years of free-air CO$_2$ enrichment. *Journal of Ecology*, *104*, 1720–1733. https://doi.org/10.1111/1365-2745.12621

Körner, C., Asshoff, R., Bignucolo, O., Hättenschwiler, S., Keel, S. G., Peláez-Riedl, S., Pepin, S., Siegwolf, R. T., & Zotz, G. (2005). Carbon flux and growth in mature deciduous forest trees exposed to elevated CO_2. *Science*, *309*, 1360–1362. https://doi.org/10.1126/science.1113977

Körner, C., Morgan, J., & Norby, R. (2007). Chapter 2: CO_2 fertilization: When, where, how much? In J. G. Canadell, D. E. Pataki, & L. F. Pitelka (Eds.), *Terrestrial ecosystems in a changing world* (pp. 9–21). Springer. https://doi.org/10.1007/978-3-540-32730-1_2

Leavitt, S. W., Paul, E. A., Galadima, A., Nakayama, F. S., Danzer, S. R., Johnson, H., & Kimball, B. A. (1995). Carbon isotopes and carbon turnover in cotton and wheat face experiments. *Plant and Soil*, *187*, 147–155. https://doi.org/10.1007/BF00017087

Leavitt, S. W., Paul, E. A., Kimball, B. A., Hendrey, G. R., Mauney, J. R., Rauschkolb, R., Rogers, H., Lewin, K. F., Nagy, J., Pinter, P. J., Jr., & Johnson, H. B. (1994). Carbon isotope dynamics of free-air CO_2-enriched cotton and soils. *Agricultural and Forest Meteorology*, *70*, 87–101. https://doi.org/10.1016/0168-1923(94)90049-3

Levin, I., Hammer, S., Kromer, B., Preunkert, S., Weller, R., & Worthy, D. E. (2022). Radiocarbon in global tropospheric carbon dioxide. *Radiocarbon*, *64*, 781–791. https://doi.org/10.1017/RDC.2021.102

Lu, X., Wang, Y. P., Luo, Y., & Jiang, L. (2018). Ecosystem carbon transit versus turnover times in response to climate warming and rising atmospheric CO_2 concentration. *Biogeosciences*, *15*, 6559–6572. https://doi.org/10.5194/bg-15-6559-2018

Luo, Y., Huang, Y., Sierra, C. A., Xia, J., Ahlström, A., Chen, Y., Hararuk, O., Hou, E., Jiang, L., Liao, C., Lu, X., Shi, Z., Smith, B., Tao, F., & Wang, Y. P. (2022). Matrix approach to land carbon cycle modeling. *Journal of Advances in Modeling Earth Systems*, *14*, e2022MS003008. https://doi.org/10.1029/2022MS003008

Luo, Y., White, L. W., Canadell, J. G., DeLucia, E. H., Ellsworth, D. S., Finzi, A., Lichter, J., & Schlesinger, W. H. (2003). Sustainability of terrestrial carbon sequestration: A case study in Duke Forest with inversion approach. *Global Biogeochemical Cycles*, *17*, 1–13. https://doi.org/10.1029/2002GB001923

Manzoni, S., Katul, G. G., & Porporato, A. (2009). Analysis of soil carbon transit times and age distributions using network theories. *Journal of Geophysical Research: Biogeosciences*, *114*, 1–14. https://doi.org/10.1029/2009JG001070

Maschler, J., Bialic-Murphy, L., Wan, J., Andresen, L. C., Zohner, C. M., Reich, P. B., Lüscher, A., Schneider, M. K., Müller, C., Moser, G., Dukes, J. S., Kappel Schmidt, I., Bilton, M., Zhu, K., & Crowther, T. W. (2022). Links across ecological scales: Plant biomass responses to elevated CO_2. *Global Change Biology*, *28*, 6115–6134. https://doi.org/10.1111/gcb.16351

Metzler, H., Müller, M., & Sierra, C. A. (2018). Transit-time and age distributions for nonlinear time-dependent compartmental systems. *Proceedings of the National Academy of Sciences of the United States of America*, *115*, 1150–1155. https://doi.org/10.1073/pnas.1705296115

Metzler, H., & Sierra, C. A. (2018). Linear autonomous compartmental models as continuous-time Markov chains: Transit-time and age distributions. *Mathematical Geosciences*, *50*, 1–34. https://doi.org/10.1007/s11004-017-9690-1

Meyer, R., Joos, F., Esser, G., Heimann, M., Hooss, G., Kohlmaier, G., Sauf, W., Voss, R., & Wittenberg, U. (1999). The substitution of high-resolution terrestrial biosphere models and carbon sequestration in response to changing CO_2 and climate. *Global Biogeochemical Cycles*, *13*, 785–802. https://doi.org/10.1029/1999GB900035

Moutinho, S. (2022). Testing the resilience of the Amazon. *Eos*, *103*, 525. https://doi.org/10.1029/2022EO220525

Muñoz, E., Chanca, I., & Sierra, C. (2023). *Transit time and age distributions of Porce model*. https://doi.org/10.5281/zenodo.8344936

Norby, R. J., DeLucia, E. H., Gielen, B., Calfapietra, C., Giardina, C. P., Kings, J. S., Ledford, J., McCarthy, H. R., Moore, D. J., Ceulemans, R., De Angelis, P., Finzi, A. C., Karnosky, D. F., Kubiske, M. E., Lukac, M., Pregitzer, K. S., Scarascia-Mugnozza, G. E., Schlesinger, W. H., & Oren, R. (2005). Forest response to elevated CO_2 is conserved across a broad range of productivity. *Proceedings of the National Academy of Sciences of the United States of America*, *102*, 18052–18056. https://doi.org/10.1073/pnas.0509478102

Paschalis, A., Katul, G. G., Fatichi, S., Palmroth, S., & Way, D. (2017). On the variability of the ecosystem response to elevated atmospheric CO_2 across spatial and temporal scales at the Duke Forest FACE experiment. *Agricultural and Forest Meteorology*, *232*, 367–383. https://doi.org/10.1016/j.agrformet.2016.09.003

Phillips, C. L., McFarlane, K. J., LaFranchi, B., Desai, A. R., Miller, J. B., & Lehman, S. J. (2015). Observations of $^{14}CO_2$ in ecosystem respiration from a temperate deciduous forest in northern Wisconsin. *Journal of Geophysical Research: Biogeosciences*, *120*, 600–616. https://doi.org/10.1002/2014JG002808

Rasmussen, M., Hastings, A., Smith, M. J., Agusto, F. B., Chen-Charpentier, B. M., Hoffman, F. M., Jiang, J., Todd-Brown, K. E., Wang, Y., Wang, Y. P., & Luo, Y. (2016). Transit times and mean ages for nonautonomous and autonomous compartmental systems. *Journal of Mathematical Biology*, *73*, 1379–1398. https://doi.org/10.1007/s00285-016-0990-8

Riederer, M., Pausch, J., Kuzyakov, Y., & Foken, T. (2015). Partitioning nee for absolute c input into various ecosystem pools by combining results from eddy-covariance, atmospheric flux partitioning and $^{13}CO_2$ pulse labeling. *Plant and Soil*, *390*, 61–76. https://doi.org/10.1007/s11104-014-2371-7

Ryan, M. G. (2013). Three decades of research at Flakaliden advancing whole-tree physiology, forest ecosystem and global change research. *Tree Physiology*, *33*, 1123–1131. https://doi.org/10.1093/treephys/tpt100

Schimel, D., Stephens, B. B., & Fisher, J. B. (2015). Effect of increasing CO_2 on the terrestrial carbon cycle. *Proceedings of the National Academy of Sciences of the United States of America*, *112*, 436–441. https://doi.org/10.1073/pnas.1407302112

Shi, Z., Allison, S. D., He, Y., Levine, P. A., Hoyt, A. M., Beem-Miller, J., Zhu, Q., Wieder, W. R., Trumbore, S., & Randerson, J. T. (2020). The age distribution of global soil carbon inferred from radiocarbon measurements. *Nature Geoscience*, *13*, 555–559. https://doi.org/10.1038/s41561-020-0596-z

Sierra, C. A., Ceballos-Núñez, V., Hartmann, H., Herrera-Ramírez, D., & Metzler, H. (2022). Ideas and perspectives: Allocation of carbon from net primary production in models is inconsistent with observations of the age of respired carbon. *Biogeosciences*, *19*, 3727–3738. https://doi.org/10.5194/bg-19-3727-2022

Sierra, C. A., Ceballos-Núñez, V., Metzler, H., & Müller, M. (2018). Representing and understanding the carbon cycle using the theory of compartmental dynamical systems. *Journal of Advances in Modeling Earth Systems*, *10*, 1729–1734. https://doi.org/10.1029/2018MS001360

Sierra, C. A., Crow, S. E., Heimann, M., Metzler, H., & Schulze, E. D. (2021). The climate benefit of carbon sequestration. *Biogeosciences*, *18*, 1029–1048. https://doi.org/10.5194/bg-18-1029-2021

Sierra, C. A., Estupinan-Suarez, L. M., & Chanca, I. (2021). The fate and transit time of carbon in a tropical forest. *Journal of Ecology*, *109*, 2845–2855. https://doi.org/10.1111/1365-2745.13723

Sierra, C. A., Hoyt, A. M., He, Y., & Trumbore, S. E. (2018). Soil organic matter persistence as a stochastic process: Age and transit time distributions of carbon in soils. *Global Biogeochemical Cycles*, *32*, 1574–1588. https://doi.org/10.1029/2018GB005950

Sierra, C. A., Müller, M., Metzler, H., Manzoni, S., & Trumbore, S. E. (2017). The muddle of ages, turnover, transit, and residence times in the carbon cycle. *Global Change Biology*, *23*, 1763–1773. https://doi.org/10.1111/gcb.13556

Smith, A. R., Lukac, M., Hood, R., Healey, J. R., Miglietta, F., & Godbold, D. L. (2013). Elevated CO_2 enrichment induces a differential biomass response in a mixed species temperate forest plantation. *New Phytologist*, *198*, 156–168. https://doi.org/10.1111/nph.12136

Steiner, C. (2008). *Biochar carbon sequestration*. http://www.biochar.org/joomla/images/stories/Steiner%20Chapter%2017%202009.pdf

Stuiver, M., & Polach, H. A. (1977). Discussion reporting of ^{14}C data. *Radiocarbon*, *19*, 355–363. https://doi.org/10.1017/S0033822200003672

Thompson, M. V., & Randerson, J. T. (1999). Impulse response functions of terrestrial carbon cycle models: Method and application. *Global Change Biology*, *5*, 371–394. https://doi.org/10.1046/j.1365-2486.1999.00235.x

Torn, M. S., & Harte, J. (2006). Missing feedbacks, asymmetric uncertainties, and the underestimation of future warming. *Geophysical Research Letters*, *33*, L10703.

Trumbore, S. (2009). Radiocarbon and soil carbon dynamics. *Annual Review of Earth and Planetary Sciences*, *37*, 47–66. https://doi.org/10.1146/annurev.earth.36.031207.124300

van Groenigen, K. J., Qi, X., Osenberg, C. W., Luo, Y., & Hungate, B. A. (2014). Faster decomposition under increased atmospheric CO_2 limits soil carbon storage. *Science*, *344*, 508–509. https://doi.org/10.1126/science.1249534

Walker, A. P., De Kauwe, M. G., Medlyn, B. E., Zaehle, S., Iversen, C. M., Asao, S., Guenet, B., Harper, A., Hickler, T., Hungate, B. A., Jain, A. K., Luo, Y., Lu, X., Lu, M., Luus, K., Megonigal, J. P., Oren, R., Ryan, E., Shu, S., … Norby, R. J. (2019). Decadal biomass increment in early secondary succession woody ecosystems is increased by CO_2 enrichment. *Nature Communications*, *10*, 454. https://doi.org/10.1038/s41467-019-08348-1

Wang, J., Xia, J., Zhou, X., Huang, K., Zhou, J., Huang, Y., Jiang, L., Xu, X., Liang, J., Wang, Y. P., Cheng, X., & Luo, Y. (2019). Evaluating the simulated mean soil carbon transit times by Earth system models using observations. *Biogeosciences*, *16*, 917–926. https://doi.org/10.5194/bg-16-917-2019

Werner, C., Meredith, L. K., Ladd, S. N., Ingrisch, J., Kübert, A., van Haren, J., Bahn, M., Bailey, K., Bamberger, I., Beyer, M., Blomdahl, D., Byron, J., Daber, E., Deleeuw, J., Dippold, M. A., Fudyma, J., Gil-Loaiza, J., Honeker, L. K., Hu, J., … Williams, J. (2021). Ecosystem fluxes during drought and recovery in an experimental forest. *Science*, *374*, 1514–1518. https://doi.org/10.1126/science.abj6789

Xiao, L., Wang, G., Wang, M., Zhang, S., Sierra, C. A., Guo, X., Chang, J., Shi, Z., & Luo, Z. (2022). Younger carbon dominates global soil carbon efflux. *Global Change Biology*, *28*, 5587–5599. https://doi.org/10.1111/gcb.16311

Zaehle, S., Medlyn, B. E., De Kauwe, M. G., Walker, A. P., Dietze, M. C., Hickler, T., Luo, Y., Wang, Y. P., El-Masri, B., Thornton, P., Jain, A., Wang, S., Warlind, D., Weng, E., Parton, W., Iversen, C. M., Gallet-Budynek, A., Mccarthy, H., Finzi, A., … Norby, R. J. (2014). Evaluation of 11 terrestrial carbon-nitrogen cycle models against observations from two temperate Free-Air CO_2 Enrichment studies. *New Phytologist*, *202*, 803–822. https://doi.org/10.1111/nph.12697

Ziegler, C., Kulawska, A., Kourmouli, A., Hamilton, L., Shi, Z., MacKenzie, A. R., Dyson, R. J., & Johnston, I. G. (2023). Quantification and uncertainty of root growth stimulation by elevated CO_2 in a mature temperate deciduous forest. *Science of the Total Environment*, *854*, 158661. https://doi.org/10.1016/j.scitotenv.2022.158661

How to cite this article: Muñoz, E., Chanca, I., & Sierra, C. A. (2023). Increased atmospheric CO_2 and the transit time of carbon in terrestrial ecosystems. *Global Change Biology*, *29*, 6441–6452. https://doi.org/10.1111/gcb.16961

APPENDIX A

A.1 | TRANSIT TIME EQUATIONS

The generalized non-linear and nonautonomous carbon cycle of an ecosystem is given by equation (Sierra, Ceballos-Núñez, et al., 2018):

$$\frac{d\mathbf{x}}{dt} = \dot{\mathbf{x}}(t) = \boldsymbol{u}(\mathbf{x}(t), t) + \mathbf{B}(\mathbf{x}(t), t) \cdot \mathbf{x}(t), \tag{A1}$$

where **x** is the carbon in each pool, ***u*** the external carbon inputs to the ecosystem from the atmosphere, and the matrix **B** the carbon cycling and transfer rates within the ecosystem. The solution of Equation (A1) is (Metzler et al., 2018):

$$\mathbf{x}(t) = \boldsymbol{\Phi}(t, t_0)\mathbf{x}^0 + \int_{t_0}^{t} \boldsymbol{\Phi}(t, t_s)\boldsymbol{u}(t_s)dt_s, \tag{A2}$$

where the matrix $\boldsymbol{\Phi}$ is the state-transition operator that describes the transport of particles through the system, $\mathbf{x}^0$ is the initial carbon content of the system at t_0, and t_s is $t - a$, with a being the carbon age. The first term of Equation (A2) indicates how much carbon remains from the initial contents, and the second term is how much remains of inputs entering after t_0 at time t (Metzler et al., 2018). The mass of carbon remaining in the ecosystem at time t with age a after photosynthetic fixation in the infinitesimal time interval dt_s is given by Equation (A3), where $\boldsymbol{f}^0$ is an initial age density distribution at initial time t_0.

$$M(t - t_s) = M(a) = \begin{cases} \boldsymbol{\Phi}(t, t_s)\boldsymbol{u}(t_s), & a < t - t_0 \\ \boldsymbol{\Phi}(t, t_0)\boldsymbol{f}^0(a - (t - t_0)), & a \geq t - t_0. \end{cases} \tag{A3}$$

The special case of Equation (1) is the linear autonomous case, expressed by the compartmental system:

$$\dot{\mathbf{x}}(t) = \boldsymbol{u} + \mathbf{B}\mathbf{x}(t). \tag{A4}$$

This system at equilibrium has steady-state carbon stocks equal to:

$$\boldsymbol{x}^* = -\mathbf{B}^{-1}\boldsymbol{u}. \tag{A5}$$

As in this case, $\mathbf{B}(t)$ is a real constant matrix **B**, and the time at which carbon enters the ecosystem is irrelevant (Rasmussen et al., 2016; Sierra, Crow, et al., 2021), $\boldsymbol{\Phi} = \mathbf{e}^{(t-t_0)\boldsymbol{B}}$ and the carbon mass is (Metzler et al., 2018):

$$\mathbf{M}(t) = \mathbf{e}^{(t-t_0)\mathbf{B}}\boldsymbol{u}. \tag{A6}$$

The total respiratory loss, $R(t)$, is proportional to the amount of carbon stored at any time t, and how the carbon entering the ecosystem at a time t_0 is lost is represented by the function (Sierra, Estupinan-Suarez, & Chanca, 2021):

$$R(t) = -\mathbf{1}^{\mathsf{T}}\mathbf{B}\mathbf{e}^{(t-t_0)\mathbf{B}}\boldsymbol{u}. \tag{A7}$$

The transit time distribution of a linear autonomous compartmental system in equilibrium is equivalent to the explicit formula provided by Metzler and Sierra (2018), which is identical to Equation (A7) by assuming $\tau = t - t_0$ and normalizing by $\| \mathbf{u} \|$ to integrate to one (Sierra, Estupinan-Suarez, & Chanca, 2021), i.e.:

$$f_T(\tau) = -\mathbf{1}^{\mathsf{T}}\mathbf{B}\mathbf{e}^{\tau\mathbf{B}}\frac{\boldsymbol{u}}{\| \boldsymbol{u} \|}, \tag{A8}$$

where $\| \mathbf{u} \|$ is the total input mass, and the symbol $\| \cdot \|$ represents the sum of all elements inside the vector.

Here, we only describe in detail the mathematical expressions of the steady state of the linear autonomous case, for details of cases with t-dependence and x-dependence using Equations (A1–A3), see Metzler et al. (2018).